The HKU Scholars Hub    The University of Hong Kong    香港大學學術庫

| | |
|---|---|
| **Title** | **Picosecond time-resolved resonance Raman observation of the iso-CH2Cl-I and iso-CH2I-Cl photoproducts from the "photoisomerization" reactions of CH 2ICl in the solution phase** |
| **Author(s)** | **Kwok, WM; Ma, C; Parker, AW; Phillips, D; Towrie, M; Matousek, P; Zheng, X; Phillips, DL** |
| **Citation** | **Journal Of Chemical Physics, 2001, v. 114 n. 17, p. 7536-7543** |
| **Issued Date** | **2001** |
| **URL** | **http://hdl.handle.net/10722/42355** |
| **Rights** | **Creative Commons: Attribution 3.0 Hong Kong License** |

# Picosecond time-resolved resonance Raman observation of the iso-CH$_2$Cl–I and iso-CH$_2$I–Cl photoproducts from the ''photoisomerization'' reactions of CH$_2$ICl in the solution phase

Wai Ming Kwok and Chensheng Ma
*Department of Chemistry, Imperial College of Science, Technology and Medicine, London SW7 2AY, United Kingdom*

Anthony W. Parker[a]
*Central Laser Facility, CLRC Rutherford Appleton Laboratory, Chilton, Didcot, Oxfordshire OX11 0QX, United Kingdom*

David Phillips[a]
*Department of Chemistry, Imperial College of Science, Technology and Medicine, London SW7 2AY, United Kingdom*

Michael Towrie and Pavel Matousek
*Central Laser Facility, CLRC Rutherford Appleton Laboratory, Chilton, Didcot, Oxfordshire OX11 0QX, United Kingdom*

Xuming Zheng
*Department of Applied Chemistry, Zheijiang Institute of Science and Technology, Hangzhou 310033, People's Republic of China*

David Lee Phillips[a),b]
*Department of Chemistry, University of Hong Kong, Hong Kong S.A.R., People's Republic of China*

We report a preliminary picosecond Stokes time-resolved resonance Raman investigation of the initial formation and subsequent decay of the photoproduct produced following 267 nm excitation of CH$_2$ClI in acetonitrile solution. Density-functional theory computations were done for several probable photoproduct species. Comparison of these computational results and results from a recent femtosecond transient absorption study to our present picosecond resonance Raman spectra indicate that the iso-CH$_2$Cl–I species is mainly produced and associated with the ~460 nm transient absorption band. The iso-CH$_2$Cl–I species appears to decay and form appreciable amounts of the more stable iso-CH$_2$I–Cl species that is associated with a ~370 nm transient absorption band after a few hundred ps. © *2001 American Institute of Physics.* [DOI: 10.1063/1.1362178]

## I. INTRODUCTION

Polyhalomethane molecules are of chemical interest from several viewpoints. They are used as reagents in a number of reactions in synthetic chemistry like cyclopropanation of olefins and diiodomethylation of carbonyl compounds.[1–9] For instance, ultraviolet photolysis of CH$_2$I$_2$ or activation of CH$_2$I$_2$ by a Zn(Cu) couple in the Simmons–Smith reaction has found utility to produce cyclopropanated products from olefins with high stereospecificity and little competition from C–H insertion.[1–5] Polyhalomethanes like CH$_2$I$_2$, CH$_2$Br$_2$, CH$_2$BrI, CH$_2$ClI, CHBr$_3$, and CHBr$_2$Cl have been observed in the troposphere in measurable quantities and are probably important sources of reactive halogens in the atmosphere.[10–16] This has led to increasing interest in the atmospheric photochemistry and chemistry of polyhalom-ethane molecules. Polyhalomethanes are also of interest for fundamental investigations of gas and condensed phase direct photodissociation reactions.[17–55]

Ultraviolet excitation of gas-phase polyhalomethanes usually leads to a direct carbon-halogen bond breaking reaction(s).[17–29] Molecular beam anisotropy measurements show these primary reaction(s) typically occur in a time much less than the rotational period of the parent molecule[17,19–22] and photofragment translational spectroscopy experiments for CH$_2$I$_2$,[18] CH$_2$BrI,[22] and CF$_2$I$_2$,[23,24] indicate that the polyatomic photofragment typically receives large amounts of internal excitation of their rotational and vibrational degrees of freedom. Gas and solution phase resonance Raman investigations for several polyhalomethane molecules showed that the direct photodissociation reaction(s) have multidimensional reaction coordinates and Franck–Condon region dynamics that appear qualitatively consistent with a semirigid radical impulsive description of the photodissociation dynamics.[30–39]

Ultraviolet excitation, direct photoionization and radiolysis of CH$_2$I$_2$ in condensed phase environments leads to

formation of characteristic absorption bands ~385 nm (strong intensity) and ~570 nm (moderate intensity)[40–47] that have been assigned to several different probable photoproduct species like trapped electrons,[40] the CH$_2$I$_2^+$ cation[45,46] or the iso-CH$_2$I–I species.[43,44] Several femtosecond transient absorption experiments have been done to follow the formation and decay of the photoproduct species.[48–50] Although the three different femtosecond studies exhibited similar results with a fast rise followed by a fast decay and then by a slower rise, three different interpretations were given because of their differing assignments for the photoproduct species responsible for the 385 and 570 nm transient absorption bands.[48–50] A recent nanosecond transient resonance Raman and density functional theory investigation demonstrated that the iso-CH$_2$I–I species is mostly responsible for the intense ~385 nm transient absorption band.[51] Further picosecond time-resolved resonance Raman spectroscopy experiments (with ~1 ps resolution) showed that the iso-CH$_2$I–I species is produced vibrationally hot within several picoseconds and then subsequently vibrationally cools on the 4–50 ps time scale.[52] We proposed a qualitative geminate and/or near geminate recombination mechanism of the initially produced hot CH$_2$I fragment and I fragment within the solvent cage to give the hot iso-CH$_2$I–I photoproduct.[52]

Many polyhalomethane molecules exhibit characteristic transient absorption bands after ultraviolet excitation in condensed phase environments.[40–47] A combination of nanosecond transient resonance Raman experiments and density-functional theory computations has begun to be used to clearly identify and characterize the photoproduct species that give rise to these transient absorption bands for a number of polyhalomethanes containing iodine and bromine atoms.[53–56] Excitation of either A-band or B-band CHI$_3$ and CH$_2$BrI produces the same iso-CHI$_3$ and iso-CH$_2$I–Br species, respectively.[53,54] This suggests that the production of iso-polyhalomethane species does not occur for a particular transition and probably happens generally after ultraviolet excitation of $n \rightarrow \sigma^*$ transitions localized on C–X bonds in the condensed phase. The lifetime or stability of the iso-polyhalomethane species produced can vary considerably and this will likely affect the chemistry of these species. We note that we could not detect any isomer species associated with CH$_2$ClI in room temperature solutions on the nanosecond time scale[53] although the iso-CH$_2$Cl–I species was readily observed in low temperature (12 K) matrices.[43,44] A recent femtosecond transient absorption study for the ultraviolet photolysis of CH$_2$ClI in room temperature acetonitrile solutions has been reported.[57] This study observed fast formation of a strong band at 460 nm and a weaker band ~710 nm that decayed with time constant of ~100 ps. This was followed by formation of a new species that had a strong band ~370 nm (strong) and ~725 nm (weak). The first transient absorption bands (at 460 and 710 nm) were attributed to formation of the iso-CH$_2$Cl–I species which has a lifetime ~100 ps and the second transient absorption (at ~370 nm) at longer times was tentatively assigned to an ICl$^-$ species.[57]

In this paper, we report picosecond time-resolved resonance Raman experiments to investigate the identity and formation of the two photoproduct species observed in the re-

cent femtosecond transient absorption study of the ultraviolet photolysis of CH$_2$ClI in room temperature solution. We utilize the results of density functional theory computations for several proposed photoproduct species and compare them to the experimental results to identify the two photoproduct species as iso-CH$_2$Cl–I and iso-CH$_2$I–Cl. Our ps experimental results indicate the iso-CH$_2$Cl–I species is formed first within several ps via recombination within the solvent cage of the initially produced CH$_2$Cl and I photofragments. The iso-CH$_2$Cl–I species then decays to form either the more stable iso-CH$_2$I–Cl species or parent molecule via isomerization reaction(s).

## II. EXPERIMENT AND CALCULATIONS

The experiments were carried out using a ps-TR$^3$ apparatus based on optical parametric amplifiers (OPAs) described in detail elsewhere.[58] Briefly, a 800 nm pulse generated from a femtosecond Ti:Sapphire oscillator is amplified from 2 to 3 mJ at 1 kHz in a regenerative amplifier. The output from the amplifier was frequency doubled in a 2 mm type I BBO ($\beta$-barium borate) crystal to generate the 400 nm probe pulses which was also used to pump the OPA for generating the 480 nm probe pulses for TR$^3$ spectroscopy. The 267 nm pump wavelength was the third harmonic of the regenerative amplifier. Typical pump and probe pulse energies at the sample were ~5–15 $\mu$J. The time resolution was ~1 ps as determined by the duration of the laser pulses (~1 ps FWHM). The ground and excited states of trans-stilbene absorb in the region of the 267 nm pump and the 400 nm (and 480 nm) probe laser beams, respectively, and were used to determine the time zero delay between the pump and probe laser beams in the TR$^3$ experiments. The time zero was established by adjusting the optical delay between the pump and probe beams to a position where the depletion of the stilbene fluorescence was halfway to the maximum fluorescence depletion by the probe laser. The time zero accuracy was estimated to be $\pm 0.5$ ps. In order to use the laser beams more effectively in the TR$^3$ experiments and considering that the rotational reorientation dynamics are much faster than the dynamics investigated in this study, parallel polarization of the pump and probe laser beams was used rather than the magic angle polarization. The beams were focused to a spot size of around 100 $\mu$m in a jet with diameter ~500 $\mu$m. Scattered photons were collected at 90° using a parabolic aluminum mirror ($f^{\#}=0.8$, $f=4$ cm), dispersed in a triple stage spectrograph and detected by a liquid nitrogen cooled charge coupled device (CCD). Each spectrum presented here was subtracted from scaled probe-before-pump and scaled net solvent measurements in order to eliminate CH$_2$ClI ground-state Raman peaks and residual solvent Raman bands, respectively. Solvent Raman bands were used to calibrate the spectra with an estimated accuracy of $\pm 10$ cm$^{-1}$ and $\pm 20$ cm$^{-1}$ in absolute frequency for the 400 and 480 nm probes, respectively. The total acquisition time for each spectrum at each time delay was about 100 min.

CH$_2$ClI and spectroscopic grade acetonitrile solvent were obtained commercially and used without further purification. 1 liter of CH$_2$ClI ($5 \times 10^{-2}$ mol dm$^{-3}$) samples were prepared in acetonitrile. Into this solution was added several
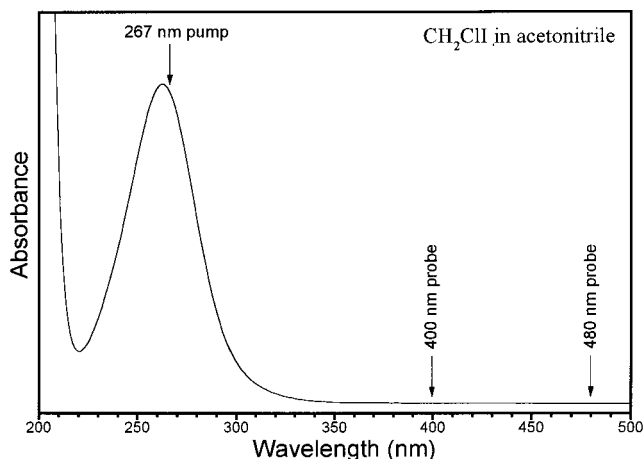
FIG. 1. Absorption spectrum of $CH_2ClI$ in acetonitrile solution with the pump and probe excitation wavelengths (in nm) for the picosecond time-resolved resonance Raman experiments shown above the spectra.

strands of copper wire to absorb the photoproduct iodine. During the experimental run the samples exhibited less than a few percent degradation as indicated by the ultraviolet (UV) absorption spectra recorded before and after the TR[3] measurement.

The GAUSSIAN program suite (G98W)[59] was used for all of the density-functional theory computations presented here and the Sadlej-PVTZ (Sadlej triple-$\zeta$ plus valence polarization) basis sets were used.[60] B3LYP (Becke three parameter with Lee, Yang, Parr functional) calculations were done to find the optimized geometry and vibrational frequencies of the species examined. Time-dependent density-functional theory at the random phase approximation computations [TD(RPA)] were used to find estimates of the electronic transition energies and oscillator strengths of the species investigated.[61]

## III. RESULTS AND DISCUSSION

Figure 1 presents the ultraviolet absorption spectrum of $CH_2ClI$ in acetonitrile solution. Figures 2 and 3 show the Stokes picosecond time-resolved resonance Raman obtained for the photoproduct(s) following 267 nm photoexcitation of $CH_2ClI$ in acetonitrile solution using 400 and 480 nm probe wavelengths, respectively. The Raman spectra appear to be composed of the fundamentals, overtones, and combination bands of several Franck–Condon active modes. Inspection of Fig. 2 shows that a Raman band $\sim 174$ cm$^{-1}$ appears first and as it decays (between 3 and 500 ps) a new Raman band $\sim 207$ cm$^{-1}$ begins to appear at later times (between 300 and 2000 ps). This suggests that a second photoproduct species is formed following decay of the first photoproduct species. The 480 nm spectrum shown in Fig. 3 appears to be mainly due to the first photoproduct species since most of the Raman band intensity decays by 300 ps and no Raman band is observed $\sim 207$ cm$^{-1}$. Table I list the vibrational frequencies of the larger Raman bands as a function of pump–probe delay time. The femtosecond transient absorption study done by Akesson and co-workers[57] on the photolysis of $CH_2ClI$ in acetonitrile solution indicates the initial photoproduct species
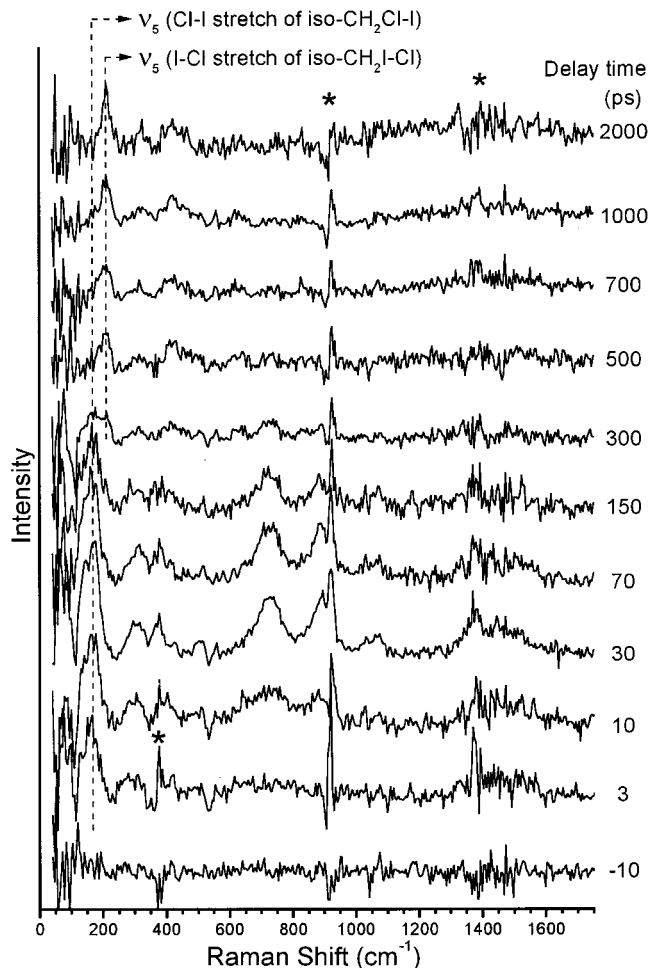


FIG. 2. Stokes picosecond time-resolved resonance Raman spectra of the photoproduct species produced from ultraviolet excitation of $CH_2ClI$ in acetonitrile solution. Spectra were obtained at varying pump (267 nm) and probe (400 nm) time delays (as indicated to the right of each spectrum). Asterisks ``*'' mark parts of the spectra where solvent subtraction artifacts are present.

is likely formed vibrationally hot. Therefore, vibrational relaxation will probably affect the Raman band intensities observed in the spectra of Figs. 2 and 3. Our previous investigation of the closely related photolysis of $CH_2I_2$ in the solution phase showed that the vibrational relaxation of the initially produced iso-$CH_2I_2$ photoproduct was essentially complete after 50–100 ps depending on the solvent used.[52] Thus we expect that vibrational relaxation will have minimal effects on the Raman band intensities observed after 100 ps in Figs. 2 and 3 where the decrease of the first photoproduct Raman band intensity and the increase of the second photoproduct Raman band intensity occurs.

In order to identify the photoproduct species we performed density-functional theory calculations to find the optimized geometry, vibrational frequencies and electronic absorption transitions for the iso-$CH_2Cl$–I, iso-$CH_2I$–Cl, $CH_2ClI^+$ cation, and $CH_2Cl$ radical species that might be produced after 267 nm excitation of the sample. Table II lists the optimized geometry of these species found from B3LYP/Sadlej-PVTZ computations. Table III compares the B3LYP/Sadlej-PVTZ computed vibrational frequencies for the prob-
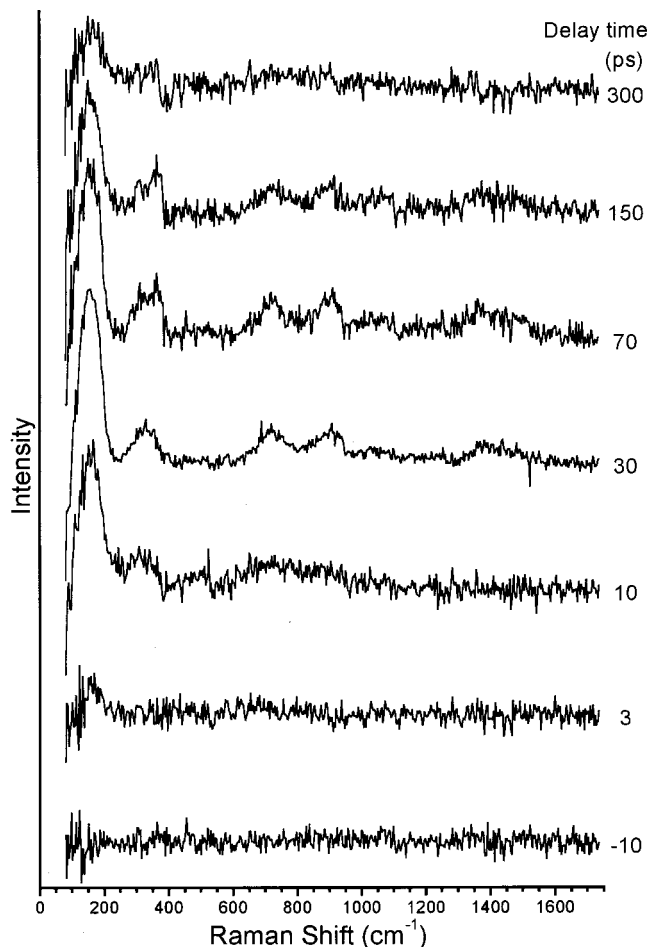
FIG. 3. Stokes picosecond time-resolved resonance Raman spectra of the photoproduct species produced from ultraviolet excitation of CH₂ICl in acetonitrile solution. Spectra were obtained at varying pump (267 nm) and probe (480 nm) time delays (as indicated to the right of each spectrum).

able photoproduct species to those of the experimental spectra for the fundamental bands. Table IV shows the B3LYP/Sadlej-PVTZ computed singlet electronic transition energies and oscillator strengths for the species given in Tables II and III.

The first photoproduct species that appears after several ps in the 400 and 480 nm probe spectra has four fundamental bands at $\sim$141, 174, 376, and 724 cm$^{-1}$ (values from the 30 ps spectrum in Fig. 2). These bands appear to have overtones and/or combination bands with each other. The four fundamental Raman bands exhibit good agreement with the computed vibrational frequencies for iso-CH₂Cl–I but not the other probable photoproduct species shown in Table III. For instance, the $\sim$141, 174, 376, and 724 cm$^{-1}$ experimental vibrational frequencies agree better with the values computed for iso-CH₂Cl–I (at 136, 194, 420, and 760 cm$^{-1}$, respectively) compared to those for iso-CH₂I–Cl (at 113, 236, 494, and 686 cm$^{-1}$, respectively). The first photoproduct species clearly shows two low-frequencies Raman bands at $\sim$141 and 174 cm$^{-1}$ that have a combination band $\sim$303 cm$^{-1}$. However, the CH₂ClI$^+$ cation has only one low frequency mode below 200 cm$^{-1}$ at $\sim$191 cm$^{-1}$ (see Table III) and can be ruled out as the species responsible for the first photoproduct resonance Raman spectra shown in Figs. 2 and

3. Similarly, the CH₂Cl radical has no low-frequency modes below 200 cm$^{-1}$ and can also be ruled out as the identity of the first photoproduct species. Inspection of Table IV shows that the computed electronic transition energies and oscillator strengths are consistent with the assignment of the first photoproduct species to the iso-CH₂Cl–I species but not the other species examined. A broad electronic transition around the 453 nm position and 0.4932 oscillator strength computed for the iso-CH₂Cl–I species is consistent with our experimental observation of the first photoproduct species using both the 480 and 400 nm probe wavelengths (albeit with differing intensities). However, the computed electronic transition energy for the iso-CH₂I–Cl species is considerably blue shifted to $\sim$332 nm and is not likely to be observed in the resonance Raman spectra obtained using 480 nm probe wavelength. Similarly, the computed electronic absorption transition energy for the CH₂ClI$^+$ cation is $\sim$489 nm with a small oscillator strength of 0.0018 and is not likely to be associated with the first photoproduct species that is more clearly observable at 400 nm that at 480 nm. The CH₂Cl radical has no singlet electronic absorption transition above 250 nm and can also be ruled out as the identity of the first photoproduct species. Comparison of our experimental results for both the vibrational frequencies and the electronic absorption transition observed in a recent femtosecond study at $\sim$460 nm[57] clearly demonstrate that the first photoproduct species is the iso-CH₂Cl–I species. This is consistent with the proposed assignment of Åkesson and co-workers.[57] Thus, we assign the vibrational fundamentals of the first photoproduct species (iso-CH₂Cl–I) as follows: The 141 cm$^{-1}$ fundamental to the $\nu_6$ C–Cl–I bend mode, the 174 cm$^{-1}$ fundamental to the $\nu_5$ Cl–I stretch mode, the 376 cm$^{-1}$ fundamental to the $\nu_9$ CH₂ twist mode, and the 724 cm$^{-1}$ fundamental to the $\nu_4$ CH₂ wag mode.

The second photoproduct species that begins to appear as the first photoproduct species disappears in the 300–500 ps region also has at least two low-frequency fundamental modes. The CH₂Cl radical can thus be ruled out as the second photoproduct species. Since there appears to be at least two fundamental vibrational modes, this also rules out the possibilities of diatomic photoproduct species like the ICl$^-$ ion or ICl molecule. The CH₂ClI$^+$ cation does not seem too likely for the following reasons: The computed 379 cm$^{-1}$ mode is fairly far away from the experimentally observed 312 cm$^{-1}$ Raman band, the computed electronic absorption transitions are also far from the experimental $\sim$370 nm transient absorption band observed for the second photoproduct species in a recent femtosecond study,[57] and the oscillator strengths for the computed electronic transitions are relatively weak. The most likely candidate for the second photoproduct is the iso-CH₂I–Cl species if we assume the 312 cm$^{-1}$ Raman band in the experimental is a combination band of two lower frequency modes as was observed in the iso-CH₂Cl–I species picosecond resonance Raman spectra. This would give a $\sim$105 cm$^{-1}$ fundamental frequency which forms a combination band with the strong 207 cm$^{-1}$ fundamental. The 105 cm$^{-1}$ fundamental can be assigned to the iso-CH₂I–Cl computed 113 cm$^{-1}$ $\nu_6$ C–I–Cl bend mode and

TABLE I. Stokes resonance Raman band vibrational frequencies (in cm$^{-1}$) observed for the picosecond resonance Raman spectra shown in Figs. 2 (400 nm probe wavelength) and 3 (480 nm probe wavelength). The solvent was acetonitrile for all of the spectra.

| Tentative vibrational assignment | (a) Iso-CH$_2$Cl–I and Iso-CH$_2$I–Cl at 400 nm probe wavelength Raman shift (in cm$^{-1}$) | | | | | | | | | |
|---|---|---|---|---|---|---|---|---|---|---|
| | 3 ps | 10 ps | 30 ps | 70 ps | 150 ps | 300 ps | 500 ps | 700 ps | 1000 ps | 2000 ps |
| Iso-CH$_2$Cl–I | | | | | | | | | | |
| $\nu_6$ | 152 | 141 | 141 | 140 | 150 | | | | | |
| $\nu_5$ | 172 | 171 | 174 | 170 | 176 | 172 | | | | |
| $\nu_5 + \nu_6 / 2\nu_5$ | 287 | 299 | 303 | 311 | 301 | 314 | | | | |
| $\nu_9$ | | 396 | 376 | 383 | 389 | | | | | |
| $\nu_4$ | | 721 | 724 | 725 | 722 | 725 | | | | |
| $\nu_4 + \nu_5$ | | 879 | 886 | 885 | 884 | 877 | | | | |
| $\nu_4 + \nu_5 + \nu_6$ | | 1059 | 1062 | 1057 | 1063 | | | | | |
| $\nu_4 + 2\nu_5 + 2\nu_6$ | | | 1373 | | | | | | | |
| $2\nu_4$ | | | 1468 | | | | | | | |
| Iso-CH$_2$I–Cl | | | | | | | | | | |
| $\nu_5$ | | | | | | 211 | 207 | 206 | 211 | 213 |
| $\nu_5 + \nu_6$ | | | | | | 314 | 312 | 316 | 323 | 322 |
| $2\nu_5$ | | | | | | 422 | 428 | 420 | 427 | 426 |

| Tentative vibrational assignment | (b) Iso-CH$_2$Cl–I at 480 nm probe wavelength Raman shift (in cm$^{-1}$) | | | | | |
|---|---|---|---|---|---|---|
| | 3 ps | 10 ps | 30 ps | 70 ps | 150 ps | 300 ps |
| | | | Iso-CH$_2$Cl–I | | | |
| $\nu_6$ | 162 | 151 | 145 | 146 | 146 | 156 |
| $\nu_5$ | 192 | 177 | 177 | 180 | 178 | 188 |
| $\nu_5\nu_6 / 2\nu_5$ | | 306 | 304 | 315 | 311 | |
| $\nu_9$ | | 342 | 340 | 363 | 363 | |
| $\nu_4$ | | 717 | 719 | 720 | 725 | |
| $\nu_4 + \nu_5$ | | 884 | 899 | 898 | 898 | |
| $\nu_4 + \nu_5 + \nu_6$ | | | 1039 | 1050 | 1056 | |
| $\nu_4 + 2\nu_5 + 2\nu_6$ | | | 1398 | 1377 | 1369 | |
| $2\nu_4$ | | | 1446 | 1490 | 1477 | |

the experimental 207 cm$^{-1}$ Raman band could be assigned to the computed 236 cm$^{-1}$ $\nu_5$ I–Cl stretch mode. The iso-CH$_2$I–Cl computed electronic transition position at 332 nm is reasonably close to the experimental transient absorption band ~370 nm observed in the femtosecond experiments[57] and the calculated oscillator strength (0.4008) for this transition is large. The B3LYP/Sadlej-PVTZ density-functional theory computational results indicate the iso-CH$_2$I–Cl species is about 4.54 kcal/mol more stable than the iso-CH$_2$Cl–I species. This is consistent with our assignment of the first photoproduct (which has a lifetime ~100 ps) to the iso-CH$_2$Cl–I species and the second photoproduct species (which has a longer lifetime on the order of hundreds of ps to nanoseconds) to the iso-CH$_2$I–Cl species. We note that this situation is similar to that found for the iso-CH$_2$Br–I and iso-CH$_2$I–Br species. The iso-CH$_2$I–Br species was computed to be more stable by ~4.1 kcal/mol and was the only species with a sufficiently long lifetime to be observed in nanosecond transient resonance Raman study.[54] We note that the assignment of the second photoproduct species to iso-CH$_2$I–Cl is not as clear cut as the first photoproduct species assignment to iso-CH$_2$Cl–I. However, the assignment of the second photoproduct to iso-CH$_2$I–Cl is consistent with the experimental and computational data available at this time.

The assignment of the second photoproduct species to iso-CH$_2$I–Cl gives rise to some interesting questions. How is iso-CH$_2$I–Cl formed? How is the C–Cl bond broken? There are two different probable scenarios for formation of the iso-CH$_2$I–Cl species. First, the initial 267 nm excitation of CH$_2$ClI could give rise to both photodissociation of the C–I bond and the C–Cl bond reaction channels (to give CH$_2$Cl+I and CH$_2$I+Cl fragments, respectively) which then undergo recombination to produce the iso-CH$_2$Cl–I and iso-CH$_2$I–Cl photoproduct species. Second, the 267 nm excitation of CH$_2$ClI results in cleavage of the C–I bond to give CH$_2$Cl+I fragments that then recombine to produce the iso-CH$_2$Cl–I species that then isomerize later to form either the more stable iso-CH$_2$I–Cl or parent CH$_2$ClI molecules. Laser flash photolysis[62] studies of the *A*-band absorption (~270 nm) of CH$_2$ClI in the gas phase showed that C–I bond cleavage is predominantly the primary reaction channel similar to *A*-band photolysis of CH$_3$I. A solution phase resonance Raman study of the *A*-band short-time photodissociation dynamics of CH$_2$ClI indicated that there is mainly motion along the C–I stretch coordinate accompanied by smaller dynamics along other coordinates and this is consistent with photodissociation of the C–I bond.[34] Inspection of the Stokes picosecond time-resolved spectra in Fig. 2 shows that there does not appear to be any Raman bands clearly attributable to the

J. Chem. Phys., Vol. 114, No. 17, 1 May 2001

Photoisomerization reactions of CH$_2$ICl    7541

TABLE II. Parameters for the optimized geometry computed from the B3LYP/Sadlej-PVTZ density-functional theory computations for the iso-CH$_2$Cl–I, iso-CH$_2$I–Cl, CH$_2$ClI$^+$, and CH$_2$Cl species. Bond lengths are in Å and bond angles are in degrees.

| Parameter | B3LYP/Sadlej-PVTZ |
|---|---|
| iso-CH$_2$Cl–I | |
| C–Cl | 1.6404 |
| C–H | 1.0914 |
| Cl–I | 2.8606 |
| Cl–C–H | 117.66 |
| H–C–H | 122.62 |
| C–Cl–I | 123.34 |
| D(H–C–Cl–I) | ±82.05 |
| iso-CH$_2$I–Cl | |
| C–I | 1.9547 |
| C–H | 1.0929 |
| I–Cl | 2.6149 |
| I–C–H | 118.52 |
| H–C–H | 119.59 |
| C–I–Cl | 120.78 |
| D(H–C–I–Cl) | ±79.61 |
| CH$_2$ClI$^+$ cation | |
| C–Cl | 1.7341 |
| C–I | 2.1887 |
| C–H | 1.1057 |
| Cl–C–I | 117.27 |
| Cl–C–H | 111.84 |
| I–C–H | 102.51 |
| H–C–H | 110.12 |
| D(Cl–C–I–H) | ±122.89 |
| CH$_2$Cl radical | |
| C–Cl | 1.7198 |
| C–H | 1.0884 |
| Cl–C–H | 117.01 |
| H–C–H | 125.43 |
| D(Cl–C–H–H) | ±171.23 |

TABLE IV. Electronic absorption transition energies and oscillator strengths (in parentheses) found from the density-functional theory computations (URPA//UB3LYP/Sadlej-PVTZ) for the iso-CH$_2$Cl–I, iso-CH$_2$I–Cl, CH$_2$ClI$^+$, and CH$_2$Cl species.

| Molecule | URPA//UB3LYP/Sadlej-PVTZ Singlet Transition Energies |
|---|---|
| Iso-CH$_2$I–Cl | |
| | 339 nm (0.0020) |
| | **332 nm (0.4008)** |
| | 270 nm (0.0067) |
| | 237 nm (0.0281) |
| | 232 nm (0.0008) |
| | 185 nm (0.0803) |
| Iso-CH$_2$Cl–I | |
| | 551 nm (0.0000) |
| | 538 nm (0.0197) |
| | **453 nm (0.4932)** |
| | 241 nm (0.0006) |
| | 234 nm (0.0206) |
| | 200 nm (0.0040) |
| CH$_2$ClI$^+$ cation | |
| | 6849 nm (0.0000) |
| | 489 nm (0.0018) |
| | 274 nm (0.0000) |
| | 247 nm (0.0013) |
| | 244 nm (0.0001) |
| | 200 nm (0.0070) |
| CH$_2$Cl radical | |
| | 224 nm (0.0024) |
| | 188 nm (0.0023) |
| | 180 nm (0.0000) |

TABLE III. Comparison of the experimental fundamental vibrational frequencies (in cm$^{-1}$) found from the time-resolved resonance Raman picosecond spectra (this work) to the calculated B3LYP/Sadlej-PVTZ density functional theory vibrational frequencies.

Ultraviolet excitation of CH$_2$ClI

| 400 nm ps-TR$^3$ 30 ps in acetonitrile Experiment | 400 nm ps-TR$^3$ 500 ps in acetonitrile Experiment | B3LYP Calc. iso-CH$_2$Cl–I Sadlej-PVTZ | | B3LYP Calc. iso-CH$_2$I–Cl Sadlej-PVTZ | | B3LYP Calc. CH$_2$ClI$^+$ cation Sadlej-PVTZ | |
|---|---|---|---|---|---|---|---|
| | | $A'$ $\nu_1$, sym. CH str. | | 3119  $A_1$ $\nu_1$, sym. CH str. | | $A'$ $\nu_1$, sym. CH str. | 3002 |
| | | $\nu_2$, CH$_2$ scissor | | 1409  $\nu_2$, CH$_2$ scissor | | $\nu_2$, CH$_2$ def. or sciss. | 1321 |
| | | $\nu_3$, C–Cl stretch | | 975  $\nu_3$, C–I stretch | | $\nu_3$, CH$_2$ wag | 1103 |
| 724 | | $\nu_4$, CH$_2$ wag | | 760  $\nu_4$, CH$_2$ wag | | $\nu_4$, C–Cl stretch | 783 |
| 174 | 207 | $\nu_5$, Cl–I stretch | | 194  $\nu_5$, I–Cl stretch | | $\nu_5$, C–I stretch | 379 |
| 141 | 105[a] | $\nu_6$, C–Cl–I bend | | 136  $\nu_6$, C–I–Cl bend | | $\nu_6$, I–C–Cl bend | 191 |
| | | $A''$ $\nu_7$, asym. CH str. | | 3276  $A''$ $\nu_7$, asym. CH str. | | $A''$ $\nu_7$, asym. CH str. | 3050 |
| | | $\nu_8$, CH$_2$ rock | | 1020  $\nu_8$, CH$_2$ rock | | $\nu_8$, CH$_2$ twist | 1050 |
| 376 | | $\nu_9$, CH$_2$ twist | | 420  $\nu_9$, CH$_2$ twist | | $\nu_9$, CH$_2$ rock | 527 |
| | | CH$_2$Cl Sadlej-PVTZ | | | | | |
| | | $A'$ $\nu_1$, CH sym. str. | 3134 | | | | |
| | | $\nu_2$, CH$_2$ def. or scissor | 1361 | | | | |
| | | $\nu_3$, C–Cl str. | 827 | | | | |
| | | $\nu_4$, CH$_2$ wag | 242 | | | | |
| | | $A''$ $\nu_5$, CH asym. str. | 3307 | | | | |
| | | $\nu_6$, CH$_2$ rock | 978 | | | | |

[a]Value obtained from subtraction of vibrational frequency for $\nu_5$ from the combination band $\nu_5 + \nu_6$ in the 500 ps 400 nm Raman spectrum. str.=stretch; sym.=symmetric; asym.=asymmetric; def.=deformation.

iso-CH$_2$I–Cl species until after 150 ps when the iso-CH$_2$Cl–I species initially formed begins to show a noticeable intensity decrease. This is consistent with recent femtosecond transient absorption results[57] which show the first photoproduct species (associated with the strong ~460 nm and weaker ~710 nm absorption bands) decays with a lifetime ~100 ps and the second photoproduct species (associated with the intense ~370 nm and weak ~725 nm absorption bands) begins to appear as the first photoproduct species decays appreciably. There seems to be a correlation between the disappearance of the first photoproduct species and the appearance of the second photoproduct species. This and the fact that only the C–I bond cleavage channel is predominantly observed following *A*-band excitation of CH$_2$ClI indicates that the second mechanism for formation of the iso-CH$_2$I–Cl photoproduct is most likely. Our results suggest that the iso-CH$_2$Cl–I photoproduct is first produced from initially formed CH$_2$Cl and I fragments via recombination within the solvent cage and then subsequently isomerize to give either the more stable iso-CH$_2$I–Cl or parent CH$_2$ClI molecules. The iso-CH$_2$I–Cl probably then decays back to the parent CH$_2$ClI molecule. Since the 267 nm photon does not have enough energy to break the C–Cl bond by itself, the isomerization of the iso-CH$_2$Cl–I product to the iso-CH$_2$I–Cl product probably proceeds via a transition state that involves concerted formation of the C–I bond, strengthening of the I–Cl bond and cleavage of the C–Cl bond. It is conceivable that the cooperative formation of the C–I bond and strengthening of the I–Cl bond as the C–Cl bond breaks would make it easier to break the C–Cl bond for the isomerisation reaction. We note that our results for CH$_2$ClI are somewhat similar to recent results reported by Reid and coworkers for OClO.[63] They photoexcited OClO and observed fast geminate recombination of the ClO and O fragments to produce a vibrationally hot OClO photoproduct that subsequently formed some ClOO with a $27.9 \pm 4.5$ ps time constant appearance time that subsequently decayed with a time constant of $398 \pm 50$ ps.[63]

It is interesting that we observed a much smaller transient resonance Raman signal for the isomer photoproducts from ultraviolet excitation of CH$_2$ClI than previously found for isomer photoproducts from excitation of CH$_2$I$_2$, CH$_2$Br$_2$, and CHI$_3$ in the solution phase.[52,64] This could be due to more efficient solvent cage escape of the CH$_2$Cl fragment initially produced by ultraviolet excitation of CH$_2$ClI in comparison to the larger and more massive CH$_2$I, CH$_2$Br, and CHI$_2$ fragments initially formed from ultraviolet excitation of CH$_2$I$_2$, CH$_2$Br$_2$, and CHI$_3$ in condensed phase environments. Molecular beam studies on ultraviolet C–X photodissociation reactions in haloalkanes and dihaloalkanes generally exhibit the trend of partitioning more of the available energy into populating modes associated with the internal degrees of freedom of the photofragments as the parent molecule becomes more massive and/or branched in structure.[65–71] Thus, the CH$_2$Cl fragment formed from CH$_2$ClI ultraviolet photodissociation would be expected to have much more translational energy than the larger and more massive CH$_2$I, CH$_2$Br, and CHI$_2$ fragments produced from corresponding photodissociation reactions of CH$_2$I$_2$,

CH$_2$Br$_2$, and CHI$_3$. This would be consistent with more fragments escaping the solvent cage for the initially produced CH$_2$Cl fragment which leads to our observing a lower signal level for the time-resolved resonance Raman spectra of the isomer species formed from solvent induced recombination. Escape of the photofragments from the solvent cage would likely produce some I-solvent contact charge transfer complexes.[72,73] The transient absorption associated with iodine atom–alkane (or cycloalkane) solvents appears to have a very broad absorption in the 300–400 nm region that has an extinction coefficient of ~1700 M$^{-1}$ cm$^{-1}$ in *n*-octane solvent[72] (Ref. 72 cautions that this value may be somewhat too high). The iodine atom–acetonitrile solvent contact charge transfer absorption band probably has a similar moderate extinction coefficient. The transient absorption bands associated with the two isomers of chloroiodomethane are very strong and on the order of 10 000 M$^{-1}$ cm$^{-1}$ or greater (see Ref. 44) and have computed oscillator strengths on the order of 0.4–0.5 (this work). Thus, one would expect the I-solvent absorption may be more difficult to observe clearly compared to the isomer–chloroiodomethane that have much stronger transitions in the 350–400 nm region. This may be part of the reason that the I-solvent transient absorption was not clearly seen in the recently reported femtosecond transient absorption study.[57] An alternative possibility is that there is not much difference in the solvent cage escape for the faster CH$_2$Cl fragment compared to CH$_2$I and CH$_2$Br fragments, but the faster CH$_2$Cl fragment has a lower quantum yield for formation of the isomer dihalomethane species than the slower and heavier fragments from photolysis of CH$_2$I$_2$ and CH$_2$BrI. This would also be consistent with the low-Raman signal observed for the iso-chlorodomethane species here and the lack of observation of the I-solvent complex transient absorption band in the femtosecond transient absorption study.[57] It is not clear how the quantum yield for formation of the isomer species depends on the translational energy of the fragments. Another possibility to be considered (though not mutually exclusive with respect to the probability of solvent cage escape taking place), is that the fast CH$_2$Cl fragment undergoes reaction with the solvent more easily than the CH$_2$I, CH$_2$Br and CHI$_2$ fragments produced in the corresponding photodissociation reactions of CH$_2$I$_2$, CH$_2$Br$_2$, and CHI$_3$. We note that halogen atom–solvent complexes absorption band position and intensity and stability of the complex can vary noticeably depending on the type of halogen atom and type of solvent.[72–76] Further work is needed to better understand how the quantum yield for solvent cage escape versus geminate (or near-geminate) recombination vary as a function of the polyhalomethane mass and substituents.

## ACKNOWLEDGMENTS

[1] H. E. Simmons and R. D. Smith, J. Am. Chem. Soc. **81**, 4256 (1959).

[2] D. C. Blomstrom, K. Herbig, and H. E. Simmons, J. Org. Chem. **30**, 959 (1965).

[3] N. J. Pienta and P. J. Kropp, J. Am. Chem. Soc. **100**, 655 (1978).

[4] P. J. Kropp, N. J. Pienta, J. A. Sawyer, and R. P. Polniaszek, Tetrahedron **37**, 3229 (1981).

[5] P. J. Kropp, Acc. Chem. Res. **17**, 131 (1984).

[6] E. C. Friedrich, J. M. Domek, and R. Y. Pong, J. Org. Chem. **50**, 4640 (1985).

[7] E. C. Freidrich, S. E. Lunetta, and E. J. Lewis, J. Org. Chem. **54**, 2388 (1989).

[8] S. Durandetti, S. Sibille, and J. Pérchon, J. Org. Chem. **56**, 3255 (1991).

[9] J. M. Concellón, P. L. Bernad, and J. A. Pérez-Andrés, Tetrahedron Lett. **39**, 1409 (1998).

[10] Th. Class and K. Ballschmiter, J. Atmos. Chem. **6**, 35 (1988).

[11] S. Klick and K. Abrahamsson, J. Geophys. Res. [Oceans] **97**, 12683 (1992).

[12] K. G. Heumann, Anal. Chim. Acta **283**, 230 (1993).

[13] R. M. Moore, M. Webb, R. Tokarczyk, and R. Wever, J. Geophys. Res., [Oceans] **101**, No. 9, 20899 (1996).

[14] J. C. Mössinger, D. E. Shallcross, and R. A. Cox, J. Chem. Soc., Faraday Trans. **94**, 1391 (1998).

[15] L. J. Carpenter, W. T. Sturges, S. A. Penkett, P. S. Liss, B. Alicke, K. Hebestreir, and U. Platt, J. Geophys. Res. [Oceans] **104**, 1679 (1999).

[16] B. Alicke, K. Hebestreit, J. Stutz, and U. Platt, Nature (London) **397**, 572 (1999).

[17] M. Kawasaki, S. J. Lee, and R. Bersohn, J. Chem. Phys. **63**, 809 (1975).

[18] G. Schmitt and F. J. Comes, J. Photochem. **14**, 107 (1980).

[19] P. M. Kroger, P. C. Demou, and S. J. Riley, J. Chem. Phys. **65**, 1823 (1976).

[20] S. J. Lee and R. Bersohn, J. Phys. Chem. **86**, 728 (1982).

[21] L. J. Butler, E. J. Hintsa, and Y. T. Lee, J. Chem. Phys. **84**, 4104 (1986).

[22] L. J. Butler, E. J. Hintsa, and Y. T. Lee, J. Chem. Phys. **86**, 2051 (1987).

[23] G. Baum, P. Felder, and J. R. Huber, J. Chem. Phys. **98**, 1999 (1993).

[24] E. A. J. Wannenmacher, P. Felder, and J. R. Huber, J. Chem. Phys. **95**, 986 (1991).

[25] W. Radloff, P. Farmanara, V. Stert, E. Schreiber, and J. R. Huber, Chem. Phys. Lett. **291**, 173 (1998).

[26] S. R. Cain, R. Hoffman, and R. Grant, J. Phys. Chem. **85**, 4046 (1981).

[27] K.-W. Jung, T. S. Ahmadi, and M. A. El-Sayed, Bull. Korean Chem. Soc. **18**, 1274 (1997).

[28] S. L. Baughcum, H. Hafmann, S. R. Leone, and D. Nesbitt, Faraday Discuss. Chem. Soc. **67**, 306 (1979).

[29] S. L. Baughcum and S. R. Leone, J. Chem. Phys. **72**, 6531 (1980).

[30] J. Zhang and D. G. Imre, J. Chem. Phys. **89**, 309 (1988).

[31] J. Zhang, E. J. Heller, D. Huber, D. G. Imre, and D. Tannor, J. Chem. Phys. **89**, 3602 (1988).

[32] W. M. Kwok and D. L. Phillips, Chem. Phys. Lett. **235**, 260 (1995).

[33] W. M. Kwok and D. L. Phillips, J. Chem. Phys. **104**, 2529 (1996).

[34] W. M. Kwok and D. L. Phillips, J. Chem. Phys. **104**, 9816 (1996).

[35] S. Q. Man, W. M. Kwok, and D. L. Phillips, J. Phys. Chem. **99**, 15705 (1995).

[36] S. Q. Man, W. M. Kwok, A. E. Johnson, and D. L. Phillips, J. Chem. Phys. **105**, 5842 (1996).

[37] F. Duschek, M. Schmitt, P. Vogt, A. Materny, and W. Kiefer, J. Raman Spectrosc. **28**, 445 (1997).

[38] M. Braun, A. Materny, M. Schmitt, W. Kiefer, and V. Engel, Chem. Phys. Lett. **284**, 39 (1998).

[39] X. Zheng and D. L. Phillips, Chem. Phys. Lett. **313**, 467 (1999).

[40] J . P. Simons and P. E. R. Tatham, J. Chem. Soc. A **1966**, 854.

[41] G. P. Brown and J. P. Simons, Trans. Faraday Soc. **65**, 3245 (1969).

[42] H. Mohan, K. N. Rao, and R. M. Iyer, Radiat. Phys. Chem. **23**, 505 (1984).

[43] G. Maier and H. P. Reisenauer, Angew. Chem. Int. Ed. Engl. **25**, 819 (1986).

[44] G. Maier, H. P. Reisenauer, J. Lu, L. J. Schaad, and B. A. Hess, Jr., J. Am. Chem. Soc. **112**, 5117 (1990).

[45] L. Andrews, F. T. Prochaska, and B. S. Ault, J. Am. Chem. Soc. **101**, 9 (1979).

[46] H. Mohan and R. M. Iyer, Radiat. Eff. **39**, 97 (1978).

[47] H. Mohan and P. N. Moorthy, J. Chem. Soc., Perkin Trans. **2**, 277 (1990).

[48] B. J. Schwartz, J. C. King, J. Z. Zhang, and C. B. Harris, Chem. Phys. Lett. **203**, 503 (1993).

[49] K. Saitow, Y. Naitoh, K. Tominaga, and Y. Yoshihara, Chem. Phys. Lett. **262**, 621 (1996).

[50] A. N. Tarnovsky, J.-L. Alvarez, A. P. Yartsev, V. Sündstrom, and E. Åkesson, Chem. Phys. Lett. **312**, 121 (1999).

[51] X. Zheng and D. L. Phillips, J. Phys. Chem. A **104**, 6880 (2000).

[52] W. M. Kwok, C. Ma, A. W. Parker, D. Phillips, M. Towrie, P. Matousek, and D. L. Phillips, J. Chem. Phys. **113**, 7471 (2000).

[53] X. Zheng and D. L. Phillips, Chem. Phys. Lett. **324**, 175 (2000).

[54] X. Zheng and D. L. Phillips, J. Chem. Phys. **113**, 3194 (2000).

[55] X. Zheng, W. M. Kwok, and D. L. Phillips, J. Phys. Chem. A **104**, 10464 (2000).

[56] X. Zheng, W.-H. Fang, and D. L. Phillips, J. Chem. Phys. **113**, 10934 (2000).

[57] A. N. Tarnovsky, M. Wall, M. Rasmusson, T. Pascher, and E. Åkesson, J. Chin. Chem. Soc. (Taipei) **47**, 769 (2000).

[58] M. Towrie, P. Matousek, A. W. Parker, and W. Shaikh, Meas. Sci. Technol. **9**, 816 (1998).

[59] M. J. Frisch, G. W. Trucks, H. B. Schlegel *et al.* GAUSSIAN 98, Revision A.7, Gaussian, Inc., Pittsburgh, PA, 1998.

[60] A. J. Sadlej, Theor. Chim. Acta **81**, 339 (1992).

[61] R. Bauernschmitt and R. Ahlrichs, Chem. Phys. Lett. **256**, 454 (1996).

[62] G. Schmitt and F. J. Comes, J. Photochem. Photobiol., A **41**, 13 (1987).

[63] C. L. Thomsen, M. P. Philpott, S. C. Hayes, and P. J. Reid, J. Chem. Phys. **112**, 505 (2000).

[64] W. M. Kwok, C. Ma, A. W. Parker, D. Phillips, M. Towrie, P. Matousek, and D. L. Phillips, J. Chem. Phys. (submitted).

[65] S. J. Riley and K. R. Wilson, Faraday Discuss. Chem. Soc. **53**, 132 (1972).

[66] C. Paterson, F. G. Godwin, and P. A. Gorry, Mol. Phys. **60**, 729 (1987).

[67] Q. Zhu, J. R. Cao, Y. Wen, J. Zhang, Y. Huang, W. Fang, and X. Wu, Chem. Phys. Lett. **144**, 486 (1988).

[68] W. K. Kang, K. W. Jung, D. C. Kim, K.-H. Jung, and H. S. Kim, Chem. Phys. **196**, 363 (1995).

[69] F. G. Godwin, C. Paterson, and P. A. Gorry, Mol. Phys. **61**, 827 (1987).

[70] T. K. Minton, P. Felder, R. J. Brudzynski, and Y. T. Lee, J. Chem. Phys. **81**, 1759 (1984).

[71] G. M. Nathanson, T. K. Minton, S. F. Shane, and Y. T. Lee, J. Chem. Phys. **90**, 6157 (1990).

[72] S. R. Logan, R. Bonneau, J. Joussot-Dubien, and P. Fornier De Violet, J. Chem. Soc., Perkin Trans. 1 **71**, 2148 (1975).

[73] P. Fornier De Violet, R. Bonneau, and J. Joussot-Dubien, J. Chim. Phys. Phys.-Chim. Biol. **70**, 1404 (1973).

[74] K. D. Raner, J. Lusztyk, and K. U. Ingold, J. Phys. Chem. **93**, 564 (1990).

[75] Z. B. Alfassi, R. E. Huie, J. P. Mittal, P. Neta, and L. C. T. Shoute, J. Phys. Chem. **97**, 9120 (1993).

[76] M. P. Philpott, S. C. Hayes, C. L. Thomsen, and P. J. Reid, Chem. Phys. **263**, 389 (2001).